

Finite and Numerical Simulations Applied in Tailor Welded Blank

Gilmar Cordeiro da Silva

Received: 14 December 2019 Accepted: 2 January 2020 Published: 15 January 2020

Abstract

The increase in economic and technological competitiveness means that the automobile industry seeks constant innovation in its production methods and processes, in order to produce lighter, safer and more efficient vehicles. Products with greater mechanical resistance, better conformability, thickness combinations of plates / materials are sought with a focus on reducing mass and increasing the rigidity of the vehicle body. In this scenario, Tailor Welded Blank (TWB), which is a top welding technique (by unconventional processes) of sheets of different specifications (materials, thicknesses and / or coatings), appears as a solution, as it allows localized distribution of mechanical properties, mass, optimizing the relationship between structural rigidity and the total weight of the vehicle body. The great challenge of this technique is to combine two processes with completely different demands, welding and mechanical forming. Due to the complexity of forming TWBs, the use of simulations has been widely adopted. In this review, different results of the numerical simulation methods used for a Tailor Welded Blank are compared, focusing on the details and the influence of the parameters used.

Index terms— numerical simulation; tailor welded blank.

1 Introduction

Tailor Welded Blank (TWB) is the combination of two or more metal sheets joined through the welding process, as shown in FIG. 1. There is possible to get a part with different materials, thicknesses, mechanical properties and coatings. This process leverages the global market in several sectors and especially the automotive market, due to the advantage of reducing production costs, weight and improving the structural performance of the vehicle. [1,2,3,8].

Source: (Adapted from ZHANG et al, 2016.) However, despite the advantages conferred by the use of TWB, their application can be considered complex, involving several variables and some complications. The most common problems are splits in the weld region, injurious levels of residual stresses, reduced formability and displacement of the weld line during forming [2,3,8].

To avoid the occurrence of failures, some adjustments are made to the dies and recently was worked finite element analysis simulations in computer. However, given the complexities of modeling conventional of TWBs, the levels of correlation are not always the best. Numerical modeling of TWBs is more complicated than the modeling of conventional sheet metal forming processes. The great difficulty in performing the numerical modeling in the TWBs conformation is due to the mechanical properties caused by the welding process, and the non-uniformity of the base materials. [3,4,5].

This paper aims to provide an overview of the use of numerical modeling techniques for different simulations in TWBs, listing the advantages and disadvantages in industrial application, as well as the challenges and research activities.

2 II.

3 Numerical Simulation Methods in Sheet Forming

The appearance of the finite element methods (FEM) occurred in the aerospace industry in the early 1950s, as a powerful numerical tool for solving mathematical engineering and physics problems, improvement the numerical resolution of a system of partial differential equations. One of the reasons why the FEM has been successful since the beginning of its formulation is its basic concept of discretization that produces many simultaneous algebraic equations that are generated and solved with the help of computers [6,7,8].

Due to the complexity of the sheet forming process, mainly in the deep-drawing operation, a fact, which led the engineers and designers, incorporate the FEM to development, seen the need to reduce the time and costs in the modelling of a new project. [6,8,55,62,63].

The representations of the effects of the contours of the elements in the sheets forming must be considered for permanent deformations and major changes in the geometry of the product. For this, it is necessary to use interpolation functions, which are curves built from known values, which in this case are the degrees of freedom of the element nodes. [6,7,9,55,62].

During the stamping of a product, the blank is subjected to a complex historical deformation and varied boundary conditions. Because of this loading history, the theory should describe the deformation of the blank that can be discretized as bi or threedimensional. Three different classes of elements can be used in the printing simulation: MEMBRANE, SHELL and SOLID [6,9].

The membrane elements have three degrees of freedom of translation per node, in the direction that two nodes are tangent and a force is normal to knot. The orientation of the normal force at the node is determined by averaging the normal forces adjacent to the element. The geometry of the sheet is adjusted through the contact of the tools. However, this method is not recommended for calculating elastic return (spring back), as it does not accurately represent the simulated values [7,9].

The shell elements have a knot with five degrees of freedom: three of translation for the two tangent vectors and the normal vector, and two rotations with the tangent vectors on the axis of rotation. The shell element is an element capable of calculating bending and has membrane characteristics. Loading in flat and perpendicular directions is allowed. All shell element formulations have an arbitrary number of integration points along the thickness of the sheet. It is recommended for all stamping operations, but it does not express accuracy for sheets of high thickness [6,7,9].

The 3D or solid elements represent all degrees of freedom and the results of a simulation with this element allow an accurate visualization of stresses and strains through the thickness and with precise spring back data. Results of a simulation with solid elements help to visualize the material's behavior in problematic regions. The disadvantage of this method is the processing time, as there are solid elements in the thickness that generate a model with many more elements, which does not happen when we use the shell elements [7,9].

4 III. Numerical Modeling Methods in

Tailor Welded Blanks

Numerical modeling in TWBs is more complicated than modeling of conventional sheet metal forming processes, mainly due to the change in mechanical and elastoplastic properties caused by the welding process and the difference in thickness between the base materials [5,10,11,12,61].

The modeling of TWBs by finite elements there are two methods: the first takes into account the weld line (TAZ -Thermally Affected Zone and WZ -Weld Zone), with a much more refined and precise mesh. The second neglects the effects of welding [13]. The first applies only in situations in which there is no localized strain of great intensity in the weld [5,11, ??4,61,62].

The simplification of the first method may cause a relative discrepancy between the practical and the simulated results. This is because in these models the Tailor Welded Blank Forming Limit Diagram (FLD) is not taken into account, but only the base materials. There is then another challenge to be overcome: prediction of the FLD of a TWB considering the local and global effects of the weld ??15,59].

The conventional methods, using stamping software (such as PAMSTAMP®, for example), there is a level of accuracy higher than 94%, which is considered excellent. When working with the stamping of TWBs, this correlation is reduced to 78%, which explains the difficulty in predicting failures [16].

There are several parameters that directly influence the numerical modeling of TWBs. Welding processes can significantly change the mechanical properties of materials in weld zone (WZ) and Heat Affected Zone (HZA). However, materials should not be considered as uniform. To survey the parameters to be adopted in the numerical simulation, the results of experimental tests are necessary, revealing the localized mechanical behavior, such as the flow limit and the plasticity parameters of the regions affected by the welding process [10,11,5].

The Plasticity is the area of mechanics that relates the calculation of stresses and strains in a body, which needs to be relatively ductile, permanently deformed by a set of applied forces. The theory is based on experimental observations on the macroscopic behavior of metals in uniform states of combined stresses. The results obtained are then idealized in mathematical equations that describe the behavior of metals under complex tensions [17,18, ??9,5,59].

102 However, it is necessary to develop more techniques that are experimental and analytical methods to
 103 quantitatively assess the mechanical characteristics of the welded metal and the formability of TWBs. Effects
 104 such as strain hardening during shaping and anisotropy of welded metal, for example, must be taken into account
 105 [20].

106 For mechanical characterization of Tailor Welded Blanks, tensile tests have been adopted, with specimens
 107 of different configurations, to feed numerical simulations and to be confronted with the so-called Mixture Rule
 108 [21,22]. In this case, we work with the ASTM E-8M standard [3].

109 The Mixtures Rule is used to extract properties from the weld, aiming to verify its influence on the mechanical
 110 properties and the elongation of the TWB. Thus, the load proportions supported by the weld and the base metal
 111 are calculated, assuming homogeneous deformation uniformity for the three materials [3,8].

112 Than those referred to mechanical effects, we also deal with micro structural issues related to welding in the
 113 Weld Zone. The changes, depending on the materials used, can be considerable. It is generated from a local
 114 softening of marten site to complex phase transformations in conditions imbalance, depending on the welded
 115 materials, the process and the welding parameters [21,23].

116 The two most used criteria in the numerical modeling of TWBs are based on the Theory of Plasticity: Yield
 117 and isotropic hardening. Different models of isotropic hardening in which the plastic deformation largely exceeds
 118 the yield, can be used in the modeling of Tailor Welded Blanks [10,11,7]. However, Holloman's equation is the
 119 simplest and most widely used model, and can be expressed as: Where: $\sigma = K \epsilon^n$ is the true stress σ $K =$ is the
 120 resistance coefficient ϵ $n =$ is the true strain $n =$ is the strain hardening coefficient After the linearization
 121 of the Holloman equation, the strain-hardening coefficient can be determined, which is a key parameter to obtain
 122 the maximum deep drawing limit in the inlay operations. The higher the strain hardening coefficient, the greater
 123 the capacity of the material to strain, without the occurrence of necking down. $\sigma = K \epsilon^n$ (1) © 2020 Global
 124 Journals

125 If there is a quantitative relationship between strain rate and yield stress, the Ludwik model can be used,
 126 which is a modification of the Holloman equation. In cold work, the yield stress is high at each strain level,
 127 mainly due to the strain-hardening phenomenon, so the yield stress is added to the equation [10,11,5]. Ludwik's
 128 law can be expressed as: $\sigma = \sigma_0 + K \epsilon^n$ (2)

129 Where: $\sigma =$ is the true stress $\sigma_0 =$ is the yield stress $K =$ is the resistance coefficient $\epsilon =$ is
 130 the true strain $n =$ is the strain hardening coefficient

131 The equations can be used so much to forming the TWBs how much for the base metal of the weld. If there
 132 is a need to consider the pre-strained material, the Ludwik model can also be modified [10,11,5]. Ludwik's law
 133 is modified and can be expressed as the Swift Equation: $\sigma = K (\epsilon + \epsilon_0)^n$ (3)

134 Where: $\sigma =$ is the true stress $\sigma_0 =$ is the yield stress $K =$ is the resistance coefficient $\epsilon =$ is
 135 is the true strain $\epsilon_0 =$ is the true strain rate $n =$ is the strain hardening coefficient A model widely used
 136 in the literature to describe the behavior of metals, such as aluminum, is the Voce equation, which takes into
 137 account the three parameters: initial yield stress, maximum stress and relaxation strain in the dynamic recovery
 138 regime. Such equation is described as: $\sigma = A \exp(-C \epsilon) + B$ (4) $C =$ is non-dimensional

139 For metals such as aluminum and ferritic stainless steels, once recovery is established, its effect is sufficiently
 140 efficient to contain hardening strain and the forming stress curve follows a horizontal line. Strains rates for both
 141 are omitted in FEM analysis of TWBs. However, one can simply take into account the effect of the strain rate,
 142 by multiplying the hardening strain law by a term like $\exp(-C \dot{\epsilon})$ [10,18,24].

143 Steel sheets, due to the rolling process, have a very significant anisotropy. This can influence data entry for
 144 numerical simulation, so it is extremely important to analyze the best yield criterion to be used in experimental
 145 tests [24,10,25,26].

146 However, the importance of anisotropy in the process of forming TWBs, the isotropic criterion of Von Mises
 147 and Gurson -Ivergaard -Needleman (GTN) are still frequently used. Von Mises formulated a flow criterion
 148 suggesting that this phenomenon occurs when the second invariant of the deviation stresses reaches a critical
 149 value. [10,12,26,27]. The Von Mises model can be expressed as: $\sigma_{eq} = \sqrt{\frac{1}{2} (\sigma_1 - \sigma_2)^2 + (\sigma_2 - \sigma_3)^2 + (\sigma_3 - \sigma_1)^2}$ (5)

150 Where: $\sigma_{eq} =$ depends on the hardening strain parameter $r =$ is the radius of the yield surface The second
 151 invariable tensor is given as: $\sigma_{ij} = \frac{1}{3} (\sigma_1 + \sigma_2 + \sigma_3) \delta_{ij} + \frac{1}{2} (\sigma_1 - \sigma_2) \delta_{12} + \frac{1}{2} (\sigma_2 - \sigma_3) \delta_{23} + \frac{1}{2} (\sigma_3 - \sigma_1) \delta_{31}$ (6)

153 Where: $\sigma_{eq} =$ is the equivalent stress $\delta_{ij} =$ is the Kronecker delta, in matrix form, corresponds to the
 154 identity matrix Hill's model is proposed for the yield of an anisotropic material and is assumed to be a quadratic
 155 function of the stress space. This is can be expressed as: $\sigma_{eq}^2 = \frac{1}{2} (\sigma_1^2 + \sigma_2^2 + \sigma_3^2) + \frac{1}{2} (\sigma_1 - \sigma_2)^2 + \frac{1}{2} (\sigma_2 - \sigma_3)^2 + \frac{1}{2} (\sigma_3 - \sigma_1)^2$ (7)

157 Where: $\sigma_1, \sigma_2, \sigma_3, \sigma_4, \sigma_5, \sigma_6 =$ are experimentally determined coefficients

158 The yield surface is defined using the three values r ($r = 0, 45, 90$) and the initial yield stress in the
 159 rolling direction [10,11,12,25,59]. If the biaxial factor is equal to 1 it is the classic Hill-48 model. Applied to flat
 160 tension the criterion can be used as:

161 In the case of normal anisotropy, the flat stress version of Hill's 1948 yield criterion can be written as: $\sigma_{eq}^2 = \frac{1}{2} (\sigma_1^2 + \sigma_2^2) + \frac{1}{2} (\sigma_1 - \sigma_2)^2 + \frac{1}{2} (\sigma_3 - \sigma_1)^2 + \frac{1}{2} (\sigma_3 - \sigma_2)^2$ (11)

163 In 1979, Hill proposed a generalized nonquadratic criterion to explain an "anomalous" observation in some
 164 aluminum alloys, where the yield forces in biaxial stress were superior to the yield forces in uniaxial stress (which

is not allowed by Hill's test 1948) [7,10,12,28]. The proposed model: $F[\sigma_1 + \sigma_2 + \sigma_3] + G[\sigma_1\sigma_2 + \sigma_1\sigma_3 + \sigma_2\sigma_3] + H[\sigma_1\sigma_2\sigma_3] + L[\sigma_1^2 + \sigma_2^2 + \sigma_3^2] + M[\sigma_1^2\sigma_2 + \sigma_1^2\sigma_3 + \sigma_2^2\sigma_1 + \sigma_2^2\sigma_3 + \sigma_3^2\sigma_1 + \sigma_3^2\sigma_2] = \sigma_y m$ (12)

Where: F, G, H, L, M, m = are experimentally determined coefficients σ_y = can be calculated from the non-linear relationship $\sigma_y = \sigma$ is the uniaxial yield stress

Other yield criteria can be derived from this model assuming combinations of experimental parameters [10]. Hosford elaborated his generalized criterion for Hill's yield and can be obtained considering $L = N = 0$. [10,28]. So for a flat isotropic material we get: $1 + R[\sigma_1 + \sigma_2 + \sigma_3] + R[R+1][\sigma_1\sigma_2 + \sigma_1\sigma_3 + \sigma_2\sigma_3] = \sigma_y m$ (13)

Where: σ_y = is the uniaxial yield stress R = is the coefficient of Lankford For a non-isotropic material, the Hosford criterion is treated by: $G[\sigma_1^2 + \sigma_2^2 + \sigma_3^2] + G[\sigma_1\sigma_2 + \sigma_1\sigma_3 + \sigma_2\sigma_3] + H[\sigma_1\sigma_2\sigma_3] = \sigma_y m$ (14)

Where: F, G, H, L, M, m = are the coefficients of Lankford σ_y = can be calculated from the non-linear relationship

The Barlat model is formulated in the stress space. The yield surface is defined using the Lankford coefficients $(\sigma_1, \sigma_2, \sigma_3)$ and the exponent m . The Barlat model was specially developed for the description of aluminum alloys. [10,19,28]. It is also a generalization of the Hosford criterion for the case where the directions of the orthotropic axes: $\sigma_1 = (3I_2 - m^2 I_3) \cos \theta + 2\sigma_2 \cos \theta + 2\sigma_3 \cos \theta + 2\sigma_2 \cos \theta + 2\sigma_3 \cos \theta + 2\sigma_2 \cos \theta + 2\sigma_3 \cos \theta$ (15)

Where: $\theta = \arccos \sqrt{2/3} \sqrt{I_2/I_3}$ with the second and third stress determining invariant (I_2, I_3) re used using Bishop-Hill notation.

5 m = represents the number of experimental r values

The yield model of Gurson Tvergaard Needleman (GTN) are generalizations of two models are the isotropic of Von Mises and Hill 1948 [10, 19,26,27,28]. For the isotropic model, we have: Where: σ_y = is the equivalent stress of Von Mises σ_y = is the yield stress of material H = is the Hydrostatic stress of material q_1, q_2, q_3 = are material parameters determined experimentally $\sigma_y = \sigma_y \sqrt{1 + q_1 \sigma_1^2 + q_2 \sigma_2^2 + q_3 \sigma_3^2} = 0$ (16) © 2020 Global Journals

For the modified criterion presenting the anisotropy parameters, we have: $\sigma_y = \sigma_y \sqrt{1 + 2q_1 \sigma_1^2 + 2q_2 \sigma_2^2 + 2q_3 \sigma_3^2} = 0$ (17)

Where:

σ_y = is the equivalent stress of Von Mises σ_y = is the yield stress of material H = is the Hydrostatic stress of material q_1, q_2, q_3 = are material parameters determined experimentally R = are the coefficients of Lankford

The numerical simulations used with this criterion are performed to describe the damage to the materials, which involves the triaxiality of the stress, that is, the law is based on the physical ductile fracture mechanism, that is, empty nucleation, growth and coalescence [5,7,10, 19,26,28].

6 IV. finite elements method for modeling of twbs

One of the main objectives in applying a virtual analysis (figure 4) is to calculate the movement of the weld line and provide an ideal force balance between the punch and blankholder. The results of this combination aim to control the flow of the blank to be forming, avoiding the movement of the weld line and thus reducing the high tensile stresses perpendicular to the weld line [29,61,62,55]. As the weld line moves to critical deep areas of inlay, the forming of the blank decreases. In some studies developed to control this situation, several tests have been carried out to decrease the strain in the thicker material, from increasing the flow of the thicker material and even reducing the stamping force on the thinner material. For that, the concept of draw beads was worked and pressure points were controlled in isolated quadrants of the blank holder [1,61,62].

Adony and Chen cited by Gautam found a strong correlation between the ductility of the weld and the limiting dome height for longitudinally welded TWBs, doing flat stretch, with original materials of similar thickness and different materials and coating combinations. The Limiting Drawing Ratio (LDR) for a TWB is between the values of the thinnest and thickest sheet if the thickness ratio is different from the unit [30,31].

According to research carried out by R. Safdarian and M. J. Torkamany, he describes that after the experimental tests carried out; the different thicknesses of the TWBs were modeled in the ABAQUS® program. The Finite Elements Method (FEM) was used to construct Forming Limit Diagram (FLD) based on the Hecker principle. In the physical cupping tests, the Limit Dome Height parameter was used, as shown in figure 5 [25].

For simulation, the following data were collected from the materials that make up the TWB: Yield Strength (YS), Ultimate Tensile Strength (UTS), hardening exponent (n), hardening coefficient (K), total elongation and anisotropy coefficient ($R_{0.2}, R_{0.45}, R_{0.90}$) [25].

In the modeling, the Punch, Die and blankholder were considered as rigid items. The TWBs were modeled as a shell element with S4R elements, maintaining the left and right side weld line inclination between 20° and 45° . The calculation of stresses and strains was based on the Hill criterion (1948) and a flat state of strain was sought. To perform the tests, the use of a 20-ton hydraulic press is suggested [25].

The experimental results show that the greater the difference in thickness and mechanical strength between the materials that make up the TWB, the greater the movement of the weld line. As a consequence, the lower the stamping of the TWB will be, which is reflected in a lower Limit Dome Height (LDH), as shown in figure ??

224 In general, the greater the difference in thickness and mechanical strength between the materials that make up
225 the TWB, the greater the movement of the weld line. Consequently, less tends to be its conformability [25].

226 According to research by Masumi, Nakajimacupping tests, tensile tests and simulations were performed to
227 correlate the values obtained experimentally. In the simulations, the effects of welding on WZ and HAZ were not
228 considered. The weld line was referred to only as the dividing point between the two materials that made up the
229 TWB. For a better correlation, it was necessary to use the anisotropy criteria and parameters [5,32].

230 In the work developed by Gautam, for the TWB, the simulation was performed on half the blank, being
231 obtained for a complete blank using the principle of symmetry on the X-Y plane, this is technique was applied
232 to reduce the size of the problem and the time of the simulation. The FEM analysis of the base material sheet
233 was also performed to compare the LDH values obtained in each case [30,31].

234 Hill's plasticity model, also known as Hill's yield potential, which is an extension of the Von Mises function
235 for anisotropic materials, was used in finite element modeling to incorporate sheets anisotropy.

236 Figure 7 shows the mesh and elements used for simulation in Gautam's work. Gautam's experimental results
237 showed that LDH is higher in the thicker sheet than in the less thick sheet, indicating greater formability of the
238 thicker sheet. Similar results were observed in the simulations, although higher LDH values were obtained in a
239 simulated manner [30,31].

240 7 Source: Adapted from Gautam et al (2019)

241 .

242 The refinement of simulations through experimental tests is of fundamental importance. The failure points
243 predicted for the FLD were captured in the DYNIFORM® software. These points were plotted as major and
244 minor strains for a comparison with the actual stress data obtained from the LDH experiments [30,31].

245 Gautam's results showed that the simulation predicts a maximum displacement value of the weld line of
246 2.45mm, which is lower than the experimental values of 2.57mm. This deviation in the results of the displacement
247 of the weld line obtained by experiments and the numerical results can be attributed to the friction between the
248 punch and the blank [30,31].

249 In another study, developed by Korouyeh in interstitial free steel sheets (IF -Interstitial Free) were used to
250 compose a TWB. The numerical investigation of the TWBs forming was done using a commercially available
251 finite element code ABAQUS 6.10 ® [60].

252 The model consisted of a hemispherical punch, blankholder, die and blank. This model was based on the
253 Hecker Forming Limit Diagram (FLD) test. Eight specimens of size 25mmx200mm to 200mmx200mm were cut
254 from the laser-welded sample, so that the weld line was perpendicular to the stretch direction (crosssectional
255 samples) [33].

256 In the standard cupping tests, the check also took place on the thinner side of the TWB and parallel to the
257 weld line. Figure 8 shows the FLD of the TWB made. It is noticed that the numerical criteria cannot predict
258 the right side of the FLD, being suitable only for the left side, under condition of plane strain. TWB samples
259 with different widths produce different LDH values, so the dispersion of the LDH test depends on the variation
260 of the stress path at the fracture site. For experiments and numerical criteria, the LDH value is minimum for a
261 125mm wide sample that is in the plane stress condition [33].

262 The comparison of the fracture position of the FEM and the experiment shows that there is good agreement
263 for the fracture position predicted by the SDT criterion and experiment. The results show that, due to the
264 increase of the sample width or in the condition of biaxial elongation, the fracture occurs closer to the weld line.

265 In research carried out by Andrade and Santos, the conditions found to be optimal in the tensile test (relative
266 inclination of the 30° and 60° weld line) were simulated. In this work, it was evidenced that the total relative
267 elongation of the weld line would support a maximum strain for an angle of 30 ° in relation to the rolling
268 direction of the base materials. The AutoForm® forming software, from the AutoForm®Company with triangular
269 meshes, Shell model, friction coefficient 0.15 was used. The materials considered were FEE 210 with 1.10mm
270 and FeP05 0.65mm, both IF. The yield criterion used was based on the Hill 1948 and the Hollomon model
271 [2,3,8,34]. According to the highlighted strain curve, it turns out that the maximum stress peak tends to decrease,
272 indicating that the purely tensile stresses are attenuated. Even that happen the weld line fractures, efforts will
273 be reduced. This indicates the relative improvement in mechanical behavior when tilting the weld line. However,
274 the simulation does not take into account the weld (HAZ and WZ), nor their mechanical properties [2,3,5,8,34].

275 In summary, there is then a lack of methods and processes that more accurately determine the effects of
276 the forming about the TWB. It is therefore necessary to develop more experimental techniques and analytical
277 methods to quantitatively evaluate the mechanical characteristics of the welded metal and the formability of
278 TWBs. Effects such as hardening strain during shaping and anisotropy of welded metal, for example, must be
279 taken into account. In this respect, the use of simulations is will growing and aims to overcome the challenges
280 mentioned above.

281 V.

8 Conclusions

282
283
284
285
286
287
288
289
290
291
292
293
294
295
296
297
298
299
300
301
302
303
304
305
306
307
308
309
310

A review of the TWBs was elaborate and in most of the work done, researchers always adopt a numerical model in their studies that disregards the WZ and the HAZ. This parameter is often adopted due to the limitations of the software's used, due to the high computational cost or the lack of experimental data for the mechanical and micro structural behavior of the weld.

Usually the elements of numerical analysis used are the shell, due to its speed of data processing and good precision. However, the inclusion of the Heat-Affected Zone (modeled also by the shell element) does not represent an improvement in the results forming and the localized Springback\effect. The reason is that due greater resistance to yield and Heat-Affected Zone modulus of the weld has an opposite effect to the elastic return.

An alternative likely would be to model the weld in 3D solid elements and the base materials by the shell element. Where the movements of the dependent nodes will be interpolated from the movement of independent nodes in the base metal mesh. The solid formulation in the region is the case where the elastic portion of the deformation is not neglected.

However, to that, there is a good approximation for numerical modeling, some conclusions are recommended: ? Previous qualification and analysis of the weld, by means of microscopy, either optical or electron beam scanning; ? The weld line must not be worked entirely parallel to the rolling direction (relative inclination of 0°), nor entirely perpendicular (relative inclination of 90°), as it tends to facilitate the propagation of cracks, splits and worsen the mechanical behavior of the TWB;

? It is necessary that the base materials work in a balance of forces ($F_A = F_B$) and, to satisfy these conditions, disregarding the metallurgical effects. This thickness ratio, the greater than the unit (1.0), the worse the forming, the threshold can be obtained by the equation: $LSR = \frac{Y_B \cdot \tan \alpha}{Y_A \cdot \tan \beta} \cdot \frac{t_{0A}}{t_{0B}}$ (18)

? The tensile tests, once the weld is qualified, proved to be useful for surveying the mechanical properties of the TWB and the influence of the relative inclination of the weld line on its performance during forming; ? Determination of an optimized curve (FLD) for the three materials, including here the weld region , which is extremely important for the development of TWBs, because with the obtaining of the curve it is possible to previously identify conditions that would lead to plastic instability or even to material failure. The validation of the numerical model requires constant comparison with experimental results, in order to identify possible deviations in the simulation results. Thus, the validation of numerical simulation has a fundamental role in this field of investigation.

lobal Journal of Researches in Engineering () Volume Xx X Issue I Ve rsion I ^{1 2}

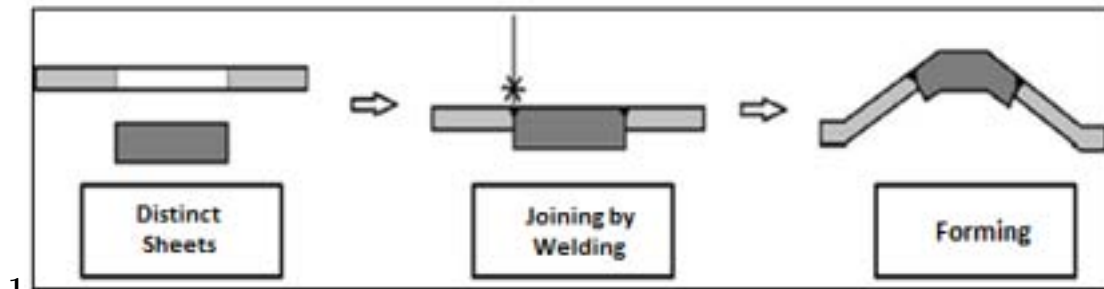
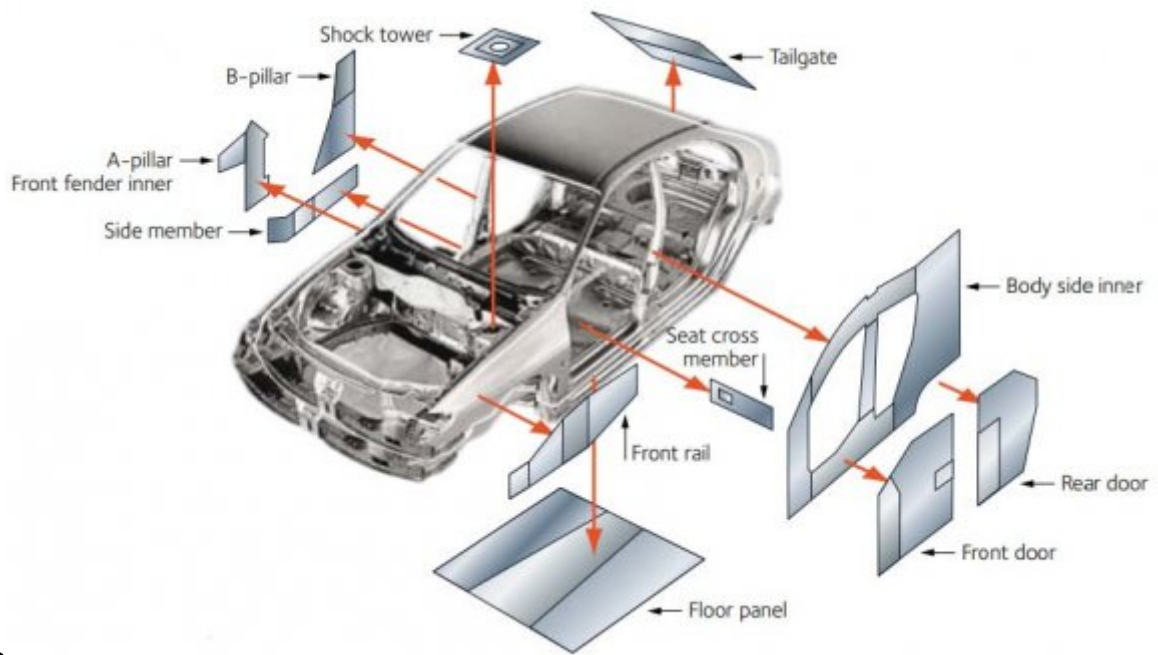


Figure 1: Figure 1 :

311

¹© 2020 Global Journals lbal Journal of Researches in Engineering () Volume Xx X Issue I Ve I Gl rsion I
²© 2020 Global Journals



2

Figure 2: Figure 2 :

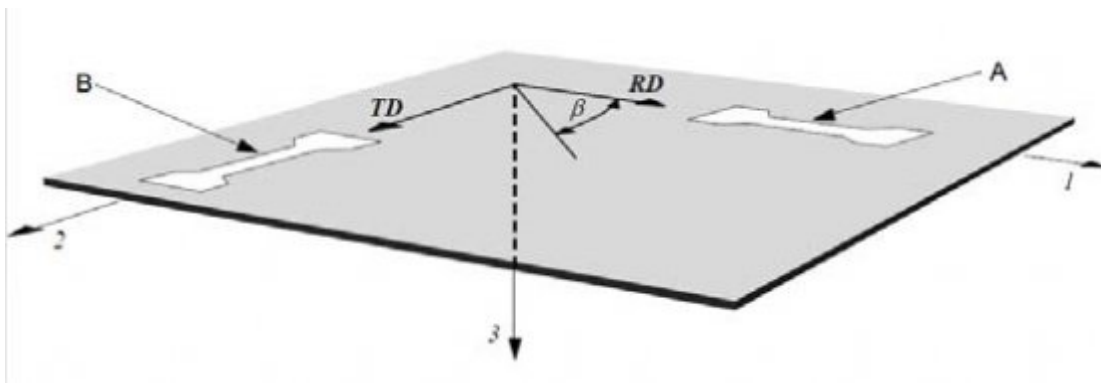


Figure 3:

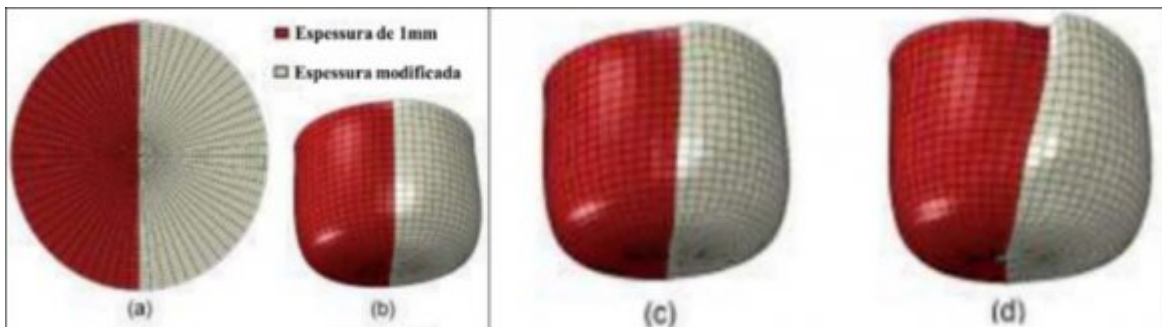
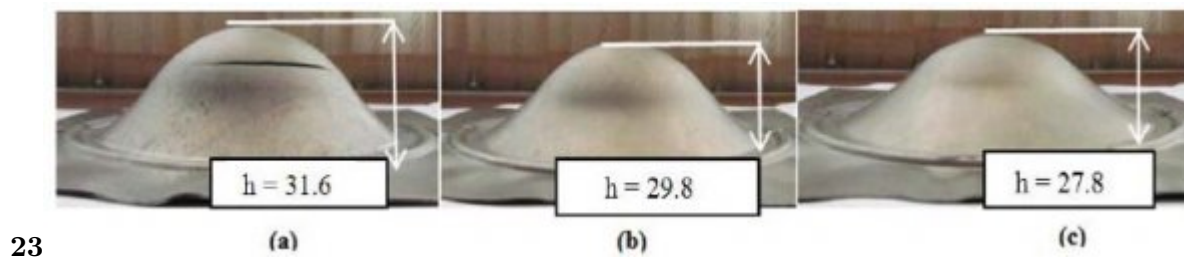


Figure 4:



23

Figure 5: 2 =Figure 3 :

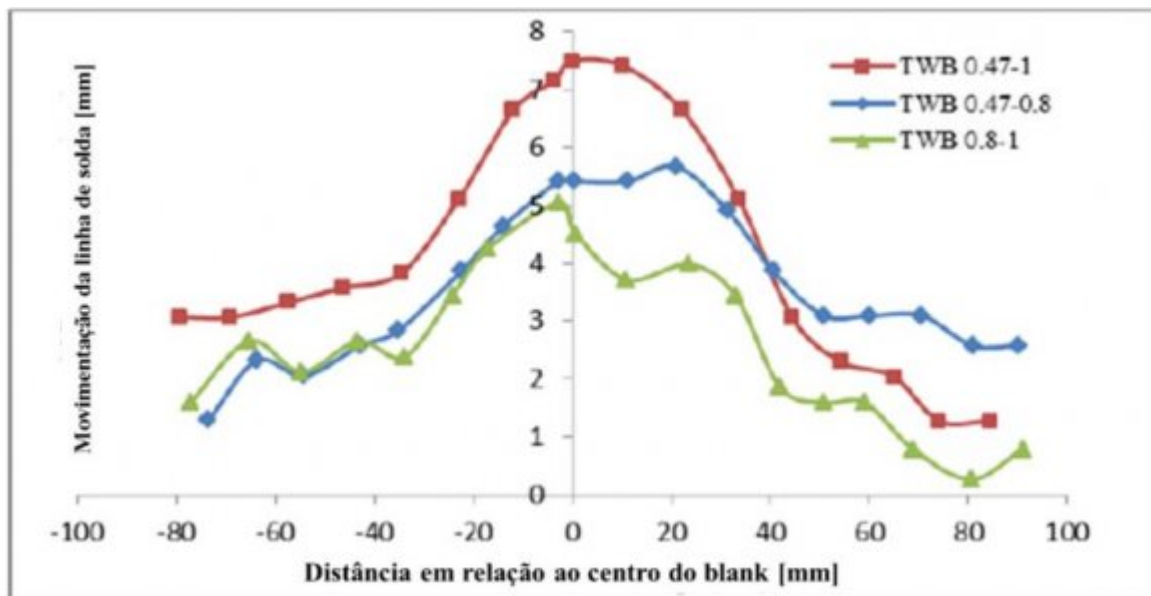


Figure 6:

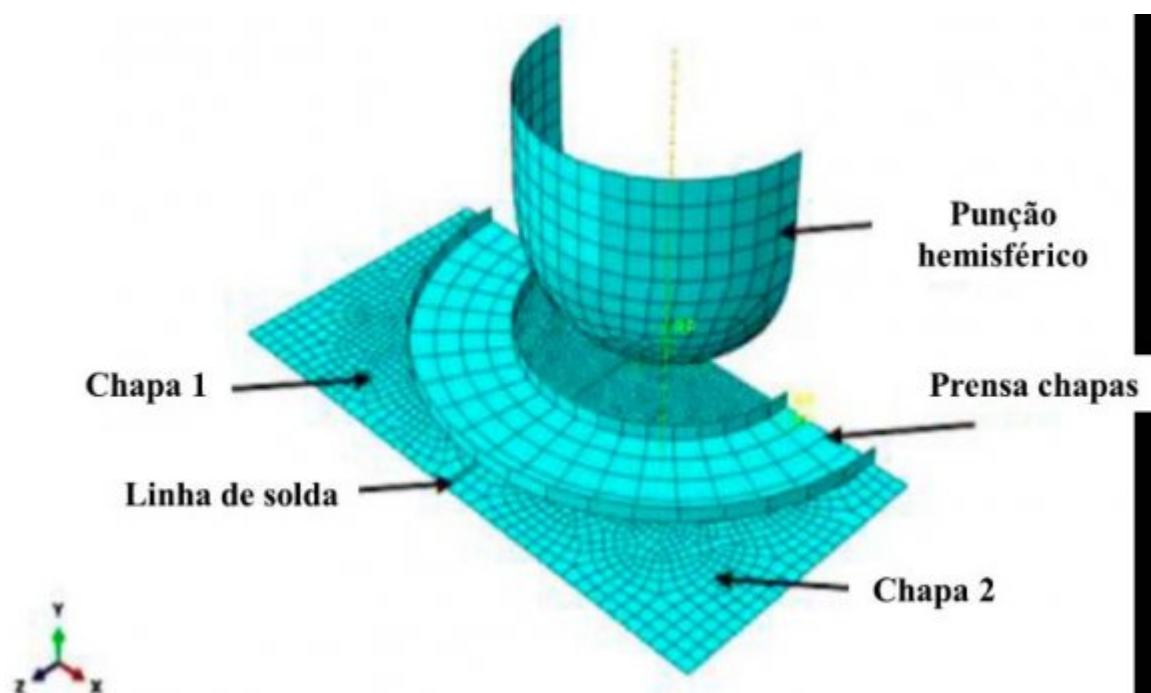
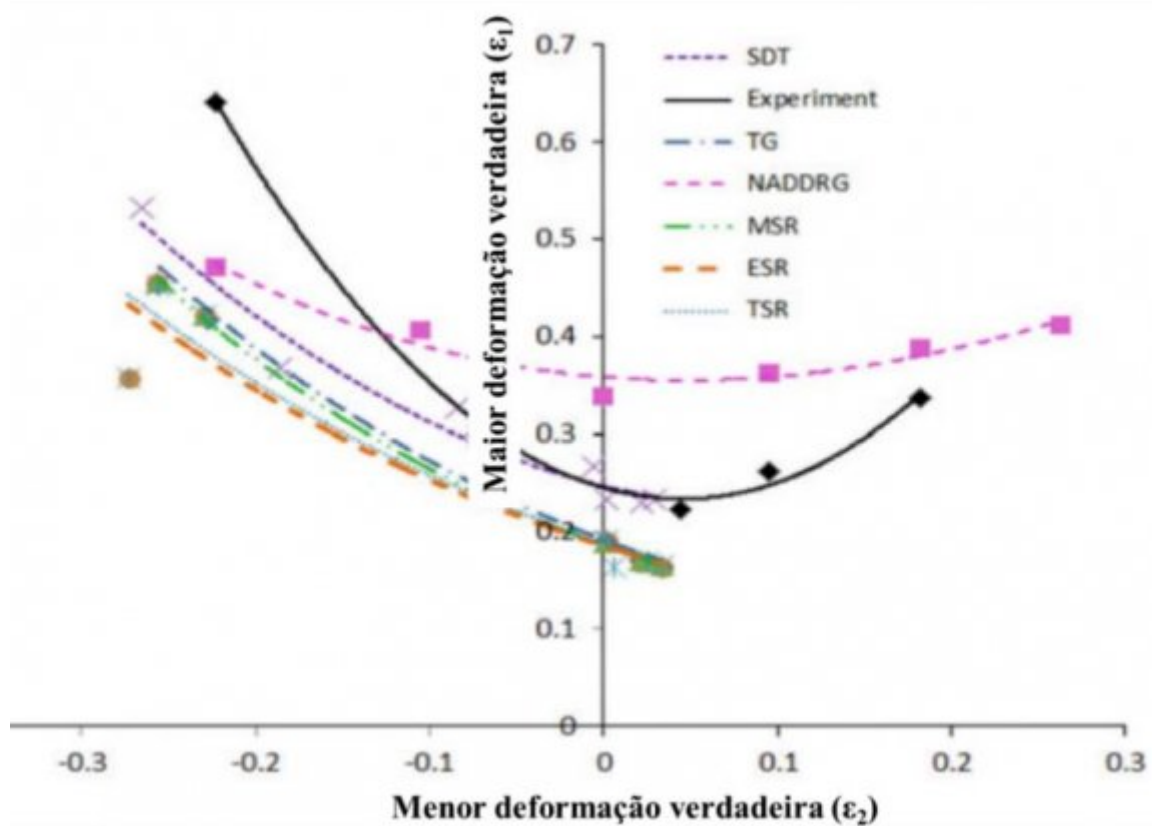
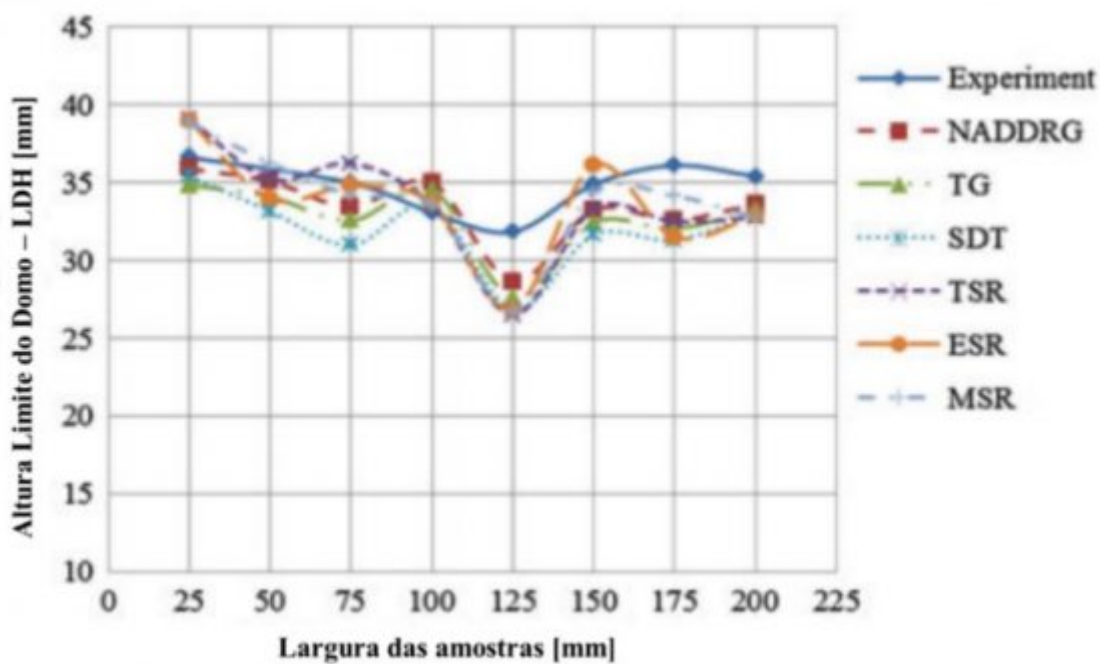


Figure 7:



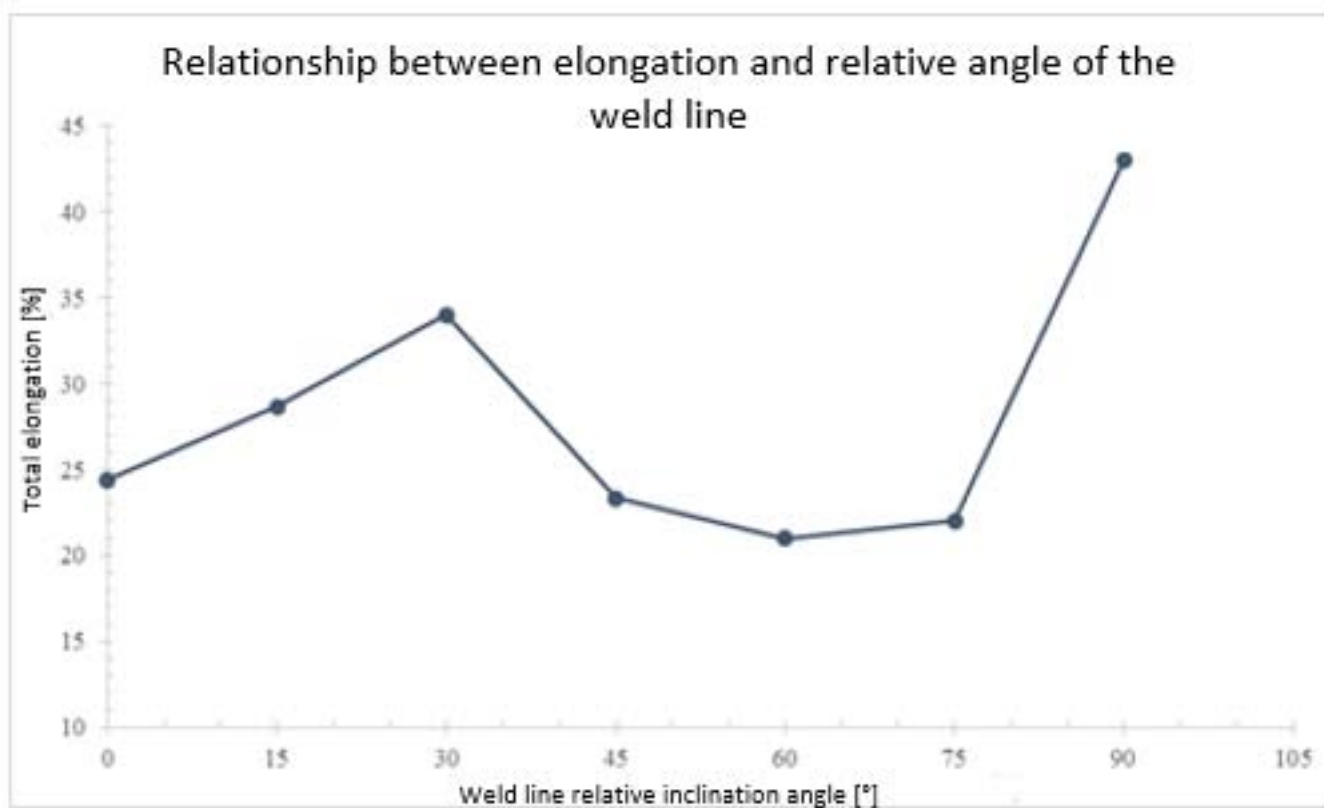
4

Figure 8: Figure 4 :



51366

Figure 9: Figure 5 : 13 Figure 6 Figure 6 :



7

Figure 10: Figure 7 :

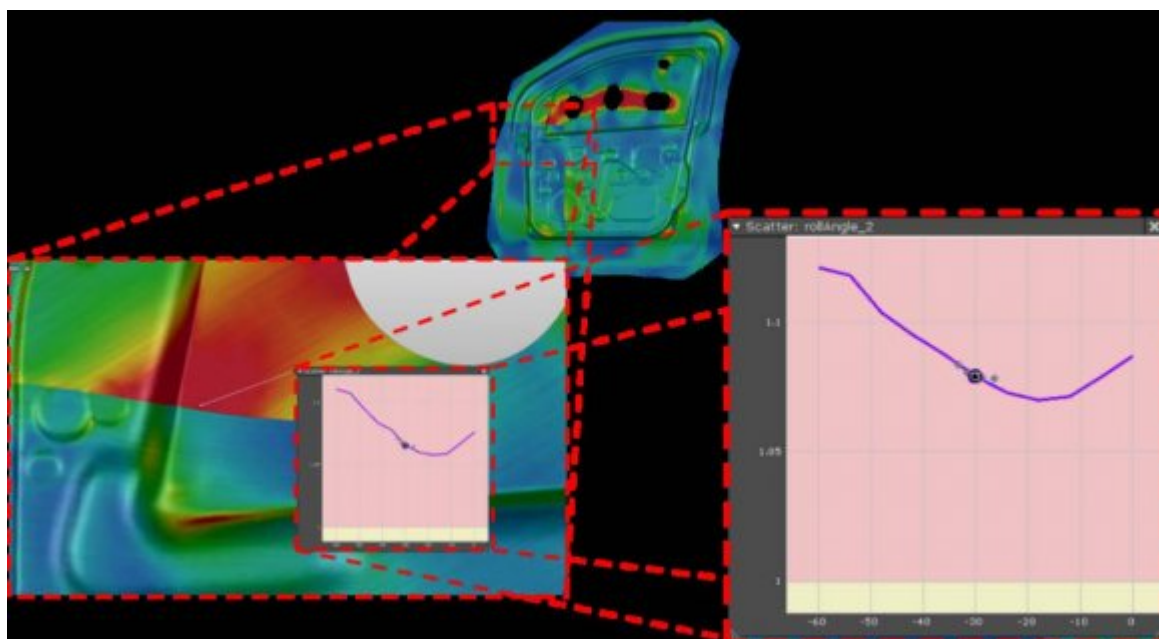


Figure 11:

312 .1 Acknowledgments

313 The authors would like to thank FIAT Chrysler do Brazil for the technical contribution to this research, Capes
314 (Coordination for the Improvement of Higher Weight) and PUC Minas (Pontifical Catholic University of Minas
315 Gerais) for financially supporting this research and for assisting in the publication of this article.

316 [Meinders et al.] , T; Meinders , Berg , Van Den .

317 [Assunção and Souza] , Guilherme Assunção , Souza .

318 [Andrade and Pereira De] , Etiene Andrade , Pereira De .

319 [Santos and Augusto Dos] , Wellington Santos , Augusto Dos .

320 [Kumar] , Amit Kumar , Rana .

321 [Datta] , Suchibrata Datta .

322 [Zadpoor] , A Zadpoor .

323 [Sinke] , J Sinke .

324 [Chan Hur] , Yong Chan Hur .

325 [Chan Hur] , Yong Chan Hur .

326 [Byung Min] , Kim Byung Min .

327 [Myoung-Gyu] , Myoung-Gyu .

328 [Moayed] , Hossein Moayed . (Roya Darabi)

329 [Ghabussi] , Aria Ghabussi .

330 [Habibi] , Mostafa Habibi .

331 [Shi et al.] , Ming F ; Shi , Ken M ; Pickett , Bhatt , K Kumar .

332 [Kumar and Ravi] , D Kumar , Ravi .

333 [Callister and Rethwisch] , William D ; Callister , David G Rethwisch .

334 [Abdelkader] , Slimane Abdelkader .

335 [Benattou Bouchouicha] , *Benattou Bouchouicha*

336 [Benguediab] , Mohamed Benguediab .

337 [Gautam et al.] , Vijay ; Gautam , Vinayak Raut , Manohar .

338 [Elsevier] , B V Elsevier . 10.1016/j.ijplas.2011.12.006. <http://dx.doi.org/10.1016/j.ijplas.2011.12.006>

340 [Duan et al.] , Duan , ; Libin , Xiao , Ning-Cong .

341 [Gong et al.] , Gong , ; Hongying , Wang , ; Sifan , Paul Knysh .

342 [Korouyeh et al.] , R Korouyeh , ; Safdarian , H Naeini , Moslemi .

343 [Lee and Nyung] , Dong Lee , Nyung .

344 [Liu and Wang] , Jun ; Liu , Li-Liang Wang .

345 [Lee et al.] , Lee , ; Junyi , Ruili Chen .

346 [Sanz] , Miguel A Sanz .

347 [Nguyen] , K Nguyen .

348 [Latorre] , Marcos Latorre .

349 [Rodríguez] , Manuel Rodríguez .

350 [Miyazak] , Yasunobu Miyazak .

351 [Sakiyama] , Tatsuya Sakiyama .

352 [Um] , Yanhong Um .

353 [Zhou] , Jing Zhou .

354 [Wang] , Baoyu Wang .

355 [Wang] , Qiaoling Wang .

356 [Ghiotti] , Andrea Ghiotti .

357 [Huynh] , G D Huynh .

358 [Zhuang] , X Zhuang .

359 [Slimaneb ()] , Sid-Ahmed Slimaneb . 2015.

8 CONCLUSIONS

- 360 [Ironmaking Steelmaking ()] , *Ironmaking & Steelmaking* 2016. Informa UK Limited. 27 p. . (s.l.), v. 45, n. 1)
- 361 [Soldagem and Inspeção ()] , & Soldagem , Inspeção . 10.1590/0104-9224/si24.32. <http://dx.doi.org/10.1590/0104-9224/si24.32> 2019. p. . (s.l.), v. 24)
- 362
- 363 [He et al. ()] ‘47. INTERNATIONAL ORGANIZATION FOR STANDARDIZATION. 6892-1: Metallic materials
- 364 -Tensile testing -Part 1: Method of test at room temperature’. He , ; Sijun , Wu , ; Xin , S Hu , Jack . *Journal*
- 365 *of Manufacturing Science and Engineering* 2003. ASME International. p. . (Formability Enhancement for
- 366 Tailor-Welded Blanks Using Blank Holding Force Control. 2 ed. Geneva: ISO, 2016. 79 p)
- 367 [Mamusi et al. (2013)] ‘A Novel Approach to the Determination of Forming Limit Diagrams for Tailor-Welded
- 368 Blanks’. Mamusi , ; Hossein , Masoumi , ; Abolfazl , Hashemi , ; Ramin , Ramazanal Mahdavinejad , R
- 369 Korouyeh , ; Safdarian , H Naeini , Moslemi . *Journal of Materials Engineering and Performance* 27 jun.
- 370 2013. Springer. 33 p. . (Nature)
- 371 [Merklein et al. ()] ‘A review on tailor blanks-Production, applications and evaluation’. Marion ; Merklein ,
- 372 Maren ; Johannes , Lechner , ; Michael , Andreas Kupert . *Journal of Materials Processing Technology* 2014.
- 373 Elsevier BV. p. . (s.l.), v. 214, n. 2)
- 374 [Shehryar Khan et al. (2020)] ‘A review on the laser welding of coated 22MnB5 press-hardened steel and its
- 375 impact on the production of tailor-welded blanks’. M Shehryar Khan , M H Razmpoosh , E Biro , & Y Zhou
- 376 . 10.1080/13621718.2020.1742472. <https://doi.org/10.1080/13621718.2020.1742472> *Science and*
- 377 *Technology of Welding and Joining* 2020. 26 Mar 2020.
- 378 [AMERICAN SOCIETY FOR TESTING AND MATERIALS. ASTM E8/E8M: Standard Test Methods for Tension Testing of M
- 379 *AMERICAN SOCIETY FOR TESTING AND MATERIALS. ASTM E8/E8M: Standard Test Methods for*
- 380 *Tension Testing of Metallic Materials*, (Conshohocken) 2016. ASTM International. 16.
- 381 [Riahi et al. ()] *Analysis of weld location effect and thickness ratio on formability of tailor welded blank. Science*
- 382 *and Technology of Welding and Joining*, M; Riahi , A Amini , J Sabbaghzadeh , M J Torkamani . 2012.
- 383 Informa UK Limited. p. . (s.l.)
- 384 [Kumar and Ravi (2016)] ‘Analytical prediction of spring back in bending of tailor-welded blanks incorporating
- 385 effect of anisotropy and weld zone properties’. D Kumar , Ravi . *Proceedings of the Institution of Mechanical*
- 386 *Engineers* 4 jan. 2016. SAGE Publications. p. . (Part L: Journal of Materials. s.l.), v. 232, n. 4)
- 387 [Singh and Kumar (2016)] ‘Application of Steel in Automotive Industry’. Mayank Singh , Kumar . *International*
- 388 *Journal of Emerging Technology and Advanced Engineering* jul. 2016. p. . (s.l.), v. 6, n. 7)
- 389 [AUTOFORM PLUS R3.1®: Software for Sheet Metal Forming. AutoForm Engineering GmbH ()]
- 390 *AUTOFORM PLUS R3.1®: Software for Sheet Metal Forming. AutoForm Engineering GmbH*, 2011.
- 391 [Li et al. (2016)] ‘Bending analysis and design optimization of tailor-rolled blank thin-walled structures with
- 392 top-hat sections’. Guangyao; Xu Li , ; Fengxiang , Chen , ; Tao , Aiguo Cheng . *International Journal Of*
- 393 *Crashworthiness* 8 nov. 2016. Informa UK Limited. p. . (s.l.), v. 22, n. 3)
- 394 [Felizardo et al.] *Caracterização Mecânica da Região Soldada de Tailor Welded Blanks (TWB) a Partir do Perfil*
- 395 *de Microdureza*, Ivanilza Felizardo , ; Felizardo , Alexandre Bracarense , Queiroz Bracarense .
- 396 [Andrade et al.] ‘Caracterização mecânica e análise de falhas de chapas fabricadas pelo processo de Tailor Welded
- 397 Blank submetidas a estampagem profunda’. Etiene Andrade , Santos Pereira De , Wellington Augusto Dos ,
- 398 ; Bracarense , Alexandre Queiroz . *ABM Proceedings*, p. . (s.l.)
- 399 [Andrade and Pereira De ()] *Caracterização mecânica e análise microestrutural de chapas obtidas pelo processo*
- 400 *de Tailor Welded Blank (TWB). 2019. 115 f. Dissertação (Mestrado) -Curso de Engenharia Mecânica*, Etiene
- 401 Andrade , Pereira De . 2019. Belo Horizonte. PPGMEC, Universidade Federal de Minas Gerais
- 402 [Andrade et al. (2019)] ‘Caracterização Mecânica e Análise Microestrutural de Chapas Obtidas pelo Processo de
- 403 Tailor Welded Blank (TWB). Soldagem & Inspeção’. Etiene Andrade , ; Pereira De , Guilherme Assunção
- 404 , ; Souza , Wellington Santos , ; Augusto Dos , Ivanilza Felizardo , ; Felizardo , Alexandre Bracarense ,
- 405 Queiroz Bracarense . 10.1590/0104-9224/si24.25. <http://dx.doi.org/10.1590/0104-9224/si24.25>
- 406 *FapUNIFESP* nov. 2019. p. . (s.l.), v. 24)
- 407 [Kumar and Nath (2007)] ‘Characterization of tensile properties of tailor welded IF steel sheets and their
- 408 formability in stretch forming’. Harish ; Kumar , A K Nath . *Journal Of Materials Processing Technology*
- 409 mar. 2007. Elsevier BV. p. . (s.l.), v. 183, n. 2-3)
- 410 [Dharan et al. (eds.) ()] *Cleavage and Ductile Fracture Mechanisms: The Microstructural Basis of Fracture*
- 411 *Toughness*, C K H Dharan , B S Kang , Iain Finnie . DHARAN, C. K. H., KANG, B. S., FINNIE, (eds.)
- 412 2016. Nova Iorque: Springer. p. . (Iain. Finnie’s Notes on Fracture Mechanics: Fundamental and Practical
- 413 Lessons)
- 414 [Suresh et al. (2016)] *Combined effect of thickness ratio and selective heating on weld line movement in stamped*
- 415 *tailor-welded blanks. Materials And Manufacturing Processes*, V V N Suresh , ; Satya , Srinivasa Regalla , ;
- 416 Prakash , Amit Gupta , Kumar . 10 nov. 2016. Informa UK Limited. p. . (s.l.), v. 32, n. 12)

- 417 [Assunção et al. (2009)] ‘Comparative study of laser welding in tailor blanks for the automotive industry’.
 418 Assunção , ; Eurico , Quintino , ; Luisa , Rosa Miranda . *The International Journal of Advanced Manufacturing*
 419 *Technology* 17 nov. 2009. Springer. p. . (s.l.), v. 49, n. 1-4)
- 420 [Filho ()] *Conformação Plástica Dos Metais. 6. ed. Campinas: Epusp, Bresciani Filho , Ettore . 2011. p. 254.*
- 421 [Huétink (2000)] ‘Deep drawing simulations of Tailor Blanks and experimental verification’ J Huétink . *Journal*
 422 *of Materials Processing Technology* jun. 2000. Elsevier BV. p. . (s.l.), v. 103, n. 1)
- 423 [Kundu (2019)] *Deformation behaviour during deep drawing operation under simple loading path: A simulation*
 424 *study*, Sanjib Kundu . 10.1016/j.matpr.2019.12.413. [https://doi.org/10.1016/j.matpr.2019.12.](https://doi.org/10.1016/j.matpr.2019.12.413)
 425 **413** 31 December 2019. Elsevier BV. (s.l), V. 2; n.3, p. 1?6)
- 426 [Karajibani et al. ()] ‘Determination of forming limit curve in two-layer metallic sheets using the finite element
 427 simulation’ Karajibani , ; Ehsan , Hashemi , ; Ramin , Mohammad Sedighi . *Proceedings of the Institution*
 428 *of Mechanical Engineers* 2016. SAGE Publications. p. . (Part L: Journal of Materials. s.l.), v. 230, n. 6)
- 429 [Kim et al. (2016)] ‘Effect of beam size in laser welding of ultra-thin stainless steel foils’ Jaehun ; Kim , Kim , ;
 430 Sanseo , Kim , ; Keunug , Jung , ; Wonyeong , Youn , ; Deokhyun , Lee , ; Jangseok , Hyungson Ki . *Journal*
 431 *Of Materials Processing Technology* jul. 2016. Elsevier BV. 233 p. . (s.l.)
- 432 [Khan et al. ()] ‘Effect of Thickness Ratio on Weld Line Displacement in Deep Drawing of Aluminium Steel
 433 Tailor Welded Blanks’ Arman ; Khan , V V N Suresh , ; Satya , Srinivasa Regalla , Prakash . *Procedia*
 434 *Materials Science* 2014. Elsevier BV. (6) p. . (s.l.)
- 435 [Li et al. ()] ‘Effects of weld line position and geometry on the formability of laser welded high strength low alloy
 436 and dual-phase steel blanks’ J Li , S S Nayak , E Biro , S K Panda , F Goodwin , Y Zhou . *Materials &*
 437 *Design* 1980-2015. 2013. Elsevier BV. 52 p. . (s.l.)
- 438 [Bui; G. Meschke and Nguyen-Xuan] *Elasto-plastic large deformation analysis of multi-patch thin shells by is*
 439 *geometric approach. Finite Elements in Analysis and Design*, H G Bui; G. Meschke , ; H Nguyen-Xuan
 440 . 10.1016/j.finel.2020.103389. fev. 2020. <https://doi.org/10.1016/j.finel.2020.103389> Elsevier
 441 BV. p. . (s.l.), v. 3, n. 2)
- 442 [Andrade and Pereira De ()] *Estudo do Efeito das Condições de Processamento Mecânico na Transformação de*
 443 *fases do aço inoxidável AISI -Centro Federal de Educação Tecnológica de Minas Gerais*, Etienne Andrade ,
 444 Pereira De . 2015. Belo Horizonte.
- 445 [Dos Reis ()] *Estudo dos Parâmetros de Influência na simulação numérica de estampagens de Chapas. Dissertação*
 446 *de Mestrado. Curso de Pós-Graduação em Engenharia Metalúrgica e de Minas*, L C Dos Reis . 2002.
- 447 [Castro and De Magalhães ()] *Estudo Numérico e Analítico das Evoluções da Força e da Espessura em Chapas*
 448 *de Aço Livre de Intersticiais Durante Processamento por Embutimento e Ironing*, Frederico Castro , De
 449 Magalhães . 2005. 2005. Belo Horizonte. 63. Dissertação (Mestrado) -Universidade Federal de Minas Gerais
- 450 [Li and Lin (2015)] ‘Experimental and Numerical Investigations of Constraint Effect on Deformation Behavior
 451 of Tailor-Welded Blanks’ Yanhua ; Li , Jianping Lin . *Journal of Materials Engineering and Performance* 30
 452 jun. 2015. Springer. p. . (s.l.), v. 24, n. 8)
- 453 [Gautam and Kumar ()] ‘Experimental and Numerical Studies on Formability of Tailor Welded Blanks of High
 454 Strength Steel’ Vijay ; Gautam , Arvind Kumar . *Procedia Manufacturing*, (edia Manufacturing) 2019.
 455 Elsevier BV. 29 p. . (s.l.)
- 456 [Vijay and Arvind Kumar (2019)] ‘Experimental and Numerical Studies on Formability of Tailor Welded Blanks
 457 of High Strength Steel’ Gautam Vijay , Arvind Kumar . *th International conference on Sheet Metal*, v.29,
 458 n.1, p472-480, feb.2019. Elsevier BV. 18.
- 459 [Zadpoor et al. ()] ‘Experimental and numerical study of machined aluminum tailor made blanks’ A A Zadpoor
 460 , J Sinke , R Benedictus . *Journal of Materials Processing Technology* 2008. 200. p. .
- 461 [Torkamany and Liaghat ()] ‘Experimental and theoretical investigation of thickness ratio effect on the forma-
 462 bility of tailor welded blank’ M J Torkamany , Gh Liaghat . *Optics & Laser Technology* 2013. Elsevier BV.
 463 51 p. . (s.l.)
- 464 [Torkamany and Liaghat ()] ‘Experimental and theoretical investigation of thickness ratio effect on the forma-
 465 bility of tailor welded blank’ M J Torkamany , Gh Liaghat . *Optics & Laser Technology* 2013. Elsevier BV.
 466 51 p. . (s.l.)
- 467 [Korkolis (2016)] ‘Experimental investigation of the mechanical response of laser-welded dissimilar blanks from
 468 advanced-and ultra-high-strength steels’ Yannis P Korkolis . *Materials & Design* jan. 2016. Elsevier BV. p.
 469 . (s.l.), v. 90)
- 470 [Zhao et al. ()] *Finite element analysis of tailor-welded blanks. Finite Elements in Analysis and Design*, K Zhao
 471 , B Chun , J K Lee . 2001. Elsevier BV. p. . (s.l.), v. 37, n. 2)
- 472 [Formability Issues in the Application of Tailor Welded Blank Sheets. Sae Technical Paper Series SAE International. 15. PANDA
 473 ‘Formability Issues in the Application of Tailor Welded Blank Sheets. Sae Technical Paper Series’ *SAE*
 474 *International. 15. PANDA*, 1 mar. 1993. p. . (s.l.. Sushanta Kumar)

8 CONCLUSIONS

- 475 [Schrek et al. (2017)] *Formability of Tailor-Welded Blanks From Dual-Phase and Bake-Hardened Steels with a*
476 *Planar Anisotropy Influence*, A Schrek , P ?vec , A Brusilová . jul. 2017. Nature: Springer. p. . (Strength Of
477 Materials, [s.l.], v. 49, n. 4)
- 478 [Safdarian (2019)] ‘Forming Limit Diagram Prediction of AISI 304-St 12.Tailor Welded Blanks Using GTN
479 Damage Model’. R Safdarian . 10.1520/JTE20180069. <https://doi.org/10.1520/JTE20180069> *Journal*
480 *of Testing and Evaluation* January 15. 2019. ASTM International. p. . (s.1], V.2, n.1)
- 481 [Cetlin and Helman ()] *Fundamentos da conformação: mecânica dos metais. 2. ed. São Paulo: Artiliber*, P R
482 Cetlin , H Helman . 2005. (265 p)
- 483 [Nalli et al. ()] ‘Global-local characterization and numerical modeling of TWB laser welded joints’. F Nalli , P
484 Spena , ; Russo , L Cortese , D Reiterer . *International Mechanical Engineering Congress and Exposition.*
485 *Flórida* 2017. 2017. 2017. ASME. 5 p. . (International Mechanical Engineering Congress and Exposition
486 -IMECE)
- 487 [Gurson-Tvergaard ()] Gurson-Tvergaard . *Needleman model of structures in carbon steel A48-AP. Brazilian*
488 *Metallurgical, Materials and Mining Association*, 2015. Elsevier BV. p. .
- 489 [Hosford and Caddell ()] William F ; Hosford , Robert M Caddell . *Metal Forming: Mechanics and Metallurgy.*
490 *3*, (Nova Iorque) 2007. Cambridge University Press. 312.
- 491 [Affonso and Amaral ()] *In: AFFONSO, Luiz Otávio Amaral. Machinery Failure Analysis Handbook: Sustain*
492 *Your Operations and Maximize Uptime*, Luiz Otávio Affonso , Amaral . 2007. Houston: Gulf Publishing
493 Company. p. . (Ductile and Brittle Fractures)
- 494 [Fazli] ‘Investigation of The Effects of Process Parameters on The Welding Line Movement in Deep Drawing of
495 Tailor Welded Blanks’. Ali Fazli . *International Journal of Advanced Design and Manufacturing Technology*
496 (9) p. . (s.l.. abr. 2016. TWB)
- 497 [Kodama and Steel ()] Shinji Kodama , Steel . *Welding Techniques for Tailor Blanks. 95. ed. Japão (Tóquio):*
498 *NSSM*, 2007. 7. (Technical Report)
- 499 [Kim (2019)] ‘MEASUREMENT OF WELD ZONE PROPERTIES OF LASER-WELDED TAILOR-WELDED
500 BLANKS AND ITS APPLICATION TO DEEP DRAWING. 2020 KSAE/ 115?08 pISSN’. Ji Hoon Kim .
501 10.1007/s12239?020?0058. <https://DOI10.1007/s12239?020?0058> *International Journal of Automotive*
502 *Technology* 30 January 2019. (s.1], V. 21; n.3, p. 615?622)
- 503 [Dieter ()] *Mechanical metallurgy. 3 Ed*, G E Dieter . 1988. Boston: McGraw-Hill.
- 504 [Zadpoor et al. ()] ‘Mechanical properties and microstructure of friction stir welded tailor-made blanks’. Amir
505 Zadpoor , ; Abbas , ; Sinke; Jos , Benedictus , ; Rinze , Raph Pieters . *Materials Science And Engineering:*
506 *A* 2008. Elsevier BV. p. . (s.l.], v. 494, n. 1-2)
- 507 [Wang et al. (2016)] ‘Multiple-iteration spring back compensation of tailor welded blanks during stamping
508 forming process’. H Wang , J Zhou , T S Zhao , L Z Liu , Q Liang . *Materials & Design* jul. 2016. 102
509 p. . (s.l.)
- 510 [Benedictus ()] *Numerical simulation modeling of tailor welded blank forming. Materials Innovation Institute*
511 *(M2i) and Delft University of Technology*, R Benedictus . 2011. 2011Woodhead. the Netherlands: Publishing
512 Limited. p. .
- 513 [Bruschi ()] *Numerical simulation of hot stamping by partition heating based on advanced constitutive modelling*
514 *of 22MnB5 behaviour. Finite Elements in Analysis and Design*, Stefania Bruschi . 2018. Elsevier BV. p. .
- 515 [Kim and Keun ()] ‘On the rule of mixtures for flow stresses in stainless-steel-clad aluminium sandwich sheet
516 metals’. Yoon Kim , Keun . 10.1007/bf01174685. <http://dx.doi.org/10.1007/bf01174685> *Springer*
517 *Science and Business Media LLC*, 1988. p. . (s.l.], v. 23, n. 2)
- 518 [Montáns ()] *Sheet metal forming analysis using a large strain anisotropic multiplicative plasticity formulation,*
519 *based on elastic correctors, which preserves the structure of the infinitesimal theory. Finite Elements in*
520 *Analysis and Design v*, Francisco J Montáns . 2019. Elsevier BV. 164 p. .
- 521 [Won-Ik et al. ()] *Simulation of molten pool dynamics and stability analysis in laser buttonhole welding.10 th*
522 *CIRP conference on Photonic Technologies*, Cho ; Won-Ik , ; Peer Woizeschke , Villads , Schultz . 2018.
523 Elsevier BV. p. .
- 524 [El-Fakir et al. ()] ‘Size-dependent mechanical properties in AA6082 tailor welded specimens’. El-Fakir , ; Omer
525 , Chen , ; Li , Lin , ; Jianguo , Trevor A Dean . *Journal of Materials Processing Technology* 2015. Elsevier
526 BV. p. . (s.l.], v. 224)
- 527 [São Paulo: LTC: GEN -Grupo Editorial Nacional ()] *São Paulo: LTC: GEN -Grupo Editorial Nacional*, 2016.
528 912. Ciência e Engenharia de (Materiais: Uma Introdução. 9)
- 529 [Kinsey and Wu ()] *Tailor welded blanks for advanced manufacturing*, Brad L ; Kinsey , Xin Wu . 2011.
530 Cambridge: Woodhead Publishing Limited. 217.

- 531 [Abdullah et al. ()] ‘Tensile testing for weld deformation properties in similar gage tailor welded blanks using
532 the rule of mixtures’. K Abdullah , P M Wild , J J Jeswiet , A Ghasempour . *Journal Of Materials Processing*
533 *Technology* 2001. Elsevier BV. p. . (s.l.), v. 112, n. 1)
- 534 [Safdarian] *The effects of strength ratio on the forming limit diagram of tailor-welded blanks*, R Safdarian .
- 535 [Li et al. (2015)] ‘Topology Optimization of an Automotive Tailor-Welded Blank Door’. Guangyao ; Li , Xu , ;
536 Fengxiang , X ; Huang , Guangyong Sun . *Journal Of Mechanical Design* 5 mar. 2015. ASME International.
537 p. . (s.l.), v. 137, n. 5)
- 538 [Brown and Bammann ()] ‘Validation of a model for static and dynamic recrystallization in metals’. Arthur A ;
539 Brown , Douglas J Bammann . *International Journal of Plasticity* 2012. p. . (s.l.)
- 540 [Kok Foong H (2020)] *Weld orientation effects on the formability of tailor welded thin steel sheets*, *ScienceDirect*,
541 Loke Kok Foong H . 10.1016/j.tws.2020.106669. <https://doi.org/10.1016/j.tws.2020.106669> 15
542 February 2020. Elsevier BV. p. . (s.l)